Driven-dissipative Euler's equations for a rigid body: A chaotic system relevant to fluid dynamics

Leaf Turner
Theoretical Division, Los Alamos National Laboratory, Los Alamos, New Mexico 87545
(Received 5 February 1996)

Adhering to the lore that vorticity is a critical ingredient of fluid turbulence, a triad of coupled helicity (vorticity) states of the incompressible Navier-Stokes fluid are followed. Effects of the remaining states of the fluid on the triad are then modeled as a simple driving term. Numerical solution of the equations yield attractors that seem strange and chaotic. This suggests that the unpredictability of nonlinear fluid dynamics (i.e., turbulence) may be traced back to the most primordial structure of the Navier-Stokes equation; namely, the driven triadic interaction. [S1063-651X(96)00911-7]

PACS number(s): 47.27.Cn, 05.45.+b, 03.20.+i, 47.52.+j

The connection between turbulence and vorticity dynamics has been much discussed [1]. We shall demonstrate that the characteristic unpredictable turbulent dynamics is already captured by the fundamental incompressible Navier-Stokes triadic interaction of three vorticity or helicity (we shall use these terms interchangeably) states, in which the effects of the remaining states are modeled as a simple driving term. We shall further demonstrate that the qualitative details of the dynamics depend crucially on the shape of the triangle formed by the three wave vectors associated with these vorticity or helicity states.

The flow velocity $\mathbf{u}(\mathbf{r},t)$ of a fluid can be represented as the superposition of a complete set of helicity states using the Chandrasekhar-Kendall representation [2]. These states are labeled by the wave vector $\mathbf{k}_i$ and the associated helicity s_i, which can take on the values of ± 1. If we isolate, from the complete set of coupled dynamical equations produced by the Navier-Stokes equation for the flow of a constant-density fluid, a set of three equations whose wave vectors satisfy $\mathbf{k}_1+\mathbf{k}_2+\mathbf{k}_3=\mathbf{0}$, we can explore the dynamics of the primordial triadic interaction. For simplicity, we shall consider the case when the spectral coefficients, $c_i(t)$, $i=1,2,3$ all have the same value of the complex phase (which we shall choose to be zero, which describes the case of real-valued spectral coefficients) [3]. Then the evolution equations for the coefficients are [4]

$$\begin{aligned}
\dot{c}_1(t)+\nu k_1^2 c_1(t)&=(s_3k_3-s_2k_2)c_2(t)c_3(t),\\
\dot{c}_2(t)+\nu k_2^2 c_2(t)&=(s_1k_1-s_3k_3)c_3(t)c_1(t),\\
\dot{c}_3(t)+\nu k_3^2 c_3(t)&=(s_2k_2-s_1k_1)c_1(t)c_2(t),
\end{aligned} \tag{1}$$

where ν is a viscous coefficient and the ''dot'' refers to a derivative with respect to time. (We have chosen the overall coupling on the right-hand side of the three equations to be unity, since any other value can be scaled away by a suitable renormalization of the c_i's.) If the $c_i(t)$'s are replaced by $L_i(t)$'s, the angular momenta along the principal axes of the moment of inertia tensor of a freely moving rigid body, if the s_ik_i's are replaced by I_i^{-1}'s, the inverse of the three principal moments of inertia, and if also ν is set equal to zero, these equations become Euler's equations of free rigid-body motion, as was noted by Waleffe [5]. A discussion of the properties of their solutions can be found in Bender and Orszag [6].

Without any driving, one notes that Eqs. (1) imply that

$$\frac{1}{2}\frac{d}{dt}\sum_{i=1}^{3} c_i^2(t)=-\nu\sum_{i=1}^{3} k_i^2 c_i^2(t)\leqslant 0,$$

so that as $t\to\infty$, $c_i(t)\to 0$, $i=1,2,3$, which is the only equilibrium solution of these equations.

Let us now assume that none of the k_i's equals zero and that

$$s_3k_3<s_2k_2<s_1k_1,$$

which implies that at least one of the quantities k_1^2 and k_3^2 is greater than k_2^2. Had we not isolated the three retained states from the complete set of states representing the fluid velocity governed by the Navier-Stokes equation, the states that we have kept would have been driven by the coupling to the other states as well as by any driving originating in the boundary conditions. In order to simulate the effects of such driving while maintaining the autonomous nature of the three evolution equations, we shall insert a driving term into the equations by reversing the sign of the linear dissipation term in the evolution equation for c_2:

$$\dot{c}_2(t)-\nu k_2^2 c_2(t)=(s_1k_1-s_3k_3)c_3(t)c_1(t).$$

Observe first that $(1/2)d/dt\Sigma_{i=1}^{3}c_i^2(t)$ is no longer negative definite, whereas the flow continues to possess a contracting volume by virtue of Eqs. (1) because

$$\sum_{i=1}^{3}\frac{\partial\dot{c}_i(t)}{\partial c_i(t)}=(-k_1^2-k_3^2+k_2^2)\nu<0.$$

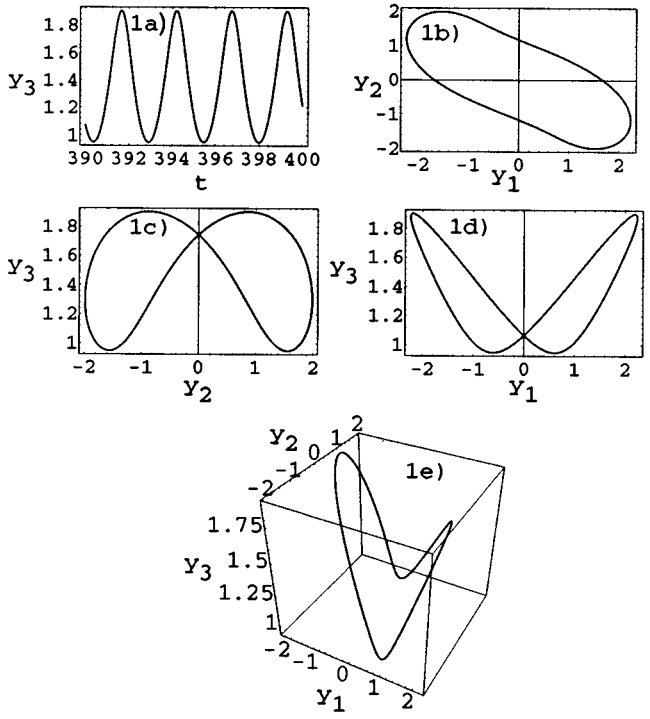

FIG. 1. The value of $\tilde{k}_1$ is set equal to the square root of the golden section ratio $(\Phi)^{1/2}$, which equals $(1.618\ldots)^{1/2}$. The values of $\tilde{k}_2$ and $\tilde{k}_3$ are 1 and $1/(\Phi)^{1/2}$, respectively. (a) y_3, exhibiting regular periodic motion, shown as a function of time after the trajectory has reached the limit cycle; (b) a projection of the limit cycle on the y_1-y_2 plane; (c) a projection of the limit cycle on the y_2-y_3 plane; (d) a projection of the limit cycle on the y_1-y_3 plane; (e) a three-dimensional plot of the limit cycle.

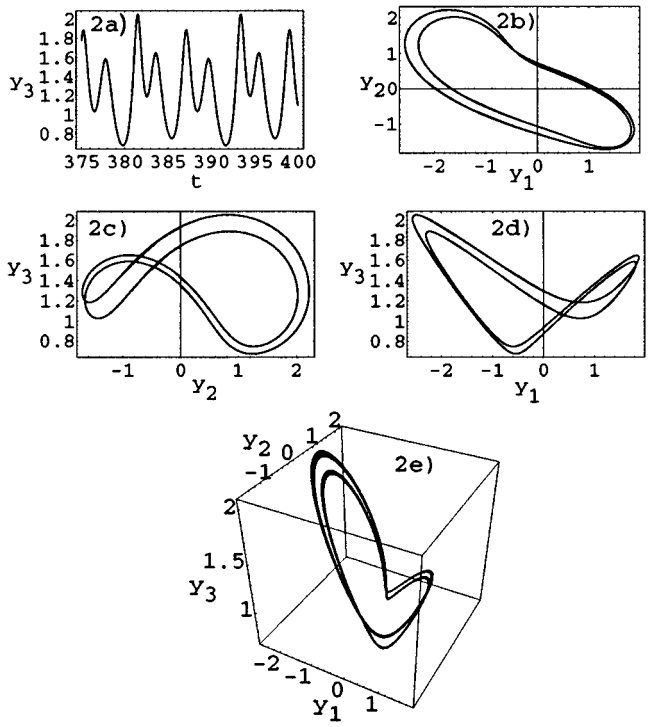

FIG. 2. The values of $\tilde{k}_1$, $\tilde{k}_2$, and $\tilde{k}_3$ are 1.33, 1, and 1/1.33, respectively. (a) y_3, exhibiting period doubling, shown as a function of time after the trajectory has reached the limit cycle; (b) a projection of the limit cycle on the y_1-y_2 plane; (c) a projection of the limit cycle on the y_2-y_3 plane; (d) a projection of the limit cycle on the y_1-y_3 plane; (e) a three-dimensional plot of the limit cycle.

Before proceeding further, we shall find it convenient to rewrite our three equations using the following definitions:

$$c_1(t)\equiv\left[\left(\frac{-\tilde{k}_2^2}{s_3k_3-s_1k_1}\right)\left(\frac{\tilde{k}_3^2}{s_1k_1-s_2k_2}\right)\right]^{1/2}y_1(t),$$

$$c_2(t)\equiv\left[\left(\frac{\tilde{k}_3^2}{s_1k_1-s_2k_2}\right)\left(\frac{\tilde{k}_1^2}{s_2k_2-s_3k_3}\right)\right]^{1/2}y_2(t),$$

$$c_3(t)\equiv\left[\left(\frac{\tilde{k}_1^2}{s_2k_2-s_3k_3}\right)\left(\frac{-\tilde{k}_2^2}{s_3k_3-s_1k_1}\right)\right]^{1/2}y_3(t);$$

where $\tilde{k}_i^2\equiv\nu k_i^2$. Then Eqs. (1) become

$$\dot{y}_1=-\tilde{k}_1^2(y_1+y_2y_3),$$

$$\dot{y}_2=\tilde{k}_2^2(y_2+y_3y_1), \tag{2}$$

$$\dot{y}_3=-\tilde{k}_3^2(y_3+y_1y_2).$$

There are five points of equilibrium, none of which is stable for arbitrary infinitesimal perturbations: (0,0,0), (1,−1,1), (−1,−1,−1), (−1,1,1), and (1,1,−1). At the origin, there is a two-dimensional stable manifold and a one-dimensional unstable manifold. If one takes the time dependence of the infinitesimal perturbations about any of the remaining four equilibrium points to be $\exp(\lambda t)$, one obtains the following characteristic equation that specifies λ:

$$\lambda^3+a_2\lambda^2+a_0=0, \tag{3}$$

where

$$a_2\equiv\tilde{k}_1^2+\tilde{k}_3^2-\tilde{k}_2^2>0, \quad a_0\equiv4\tilde{k}_1^2\tilde{k}_2^2\tilde{k}_3^2>0.$$

One may verify by Cardan's method for solving cubic equations [7] that Eq. (3) has one real negative root and two complex roots. To find the sign of the real parts of the complex roots, we set λ equal to $\gamma+i\omega$, where $\omega\neq0$. The real and imaginary parts of Eq. (3) then yield, respectively,

$$\gamma^3+a_2\gamma^2-3\omega^2\gamma-a_2\omega^2+a_0=0,$$

$$\omega^2=3\gamma^2+2a_2\gamma.$$

Eliminating ω from the first equation by means of the second leads to

$$\gamma=\frac{a_0}{2(2\gamma+a_1)^2}>0.$$

Hence, unlike the origin, each of the latter four equilibrium points of Eqs. (2) has a one-dimensional stable manifold and a two-dimensional unstable manifold. These equations also can be expressed in the following way:

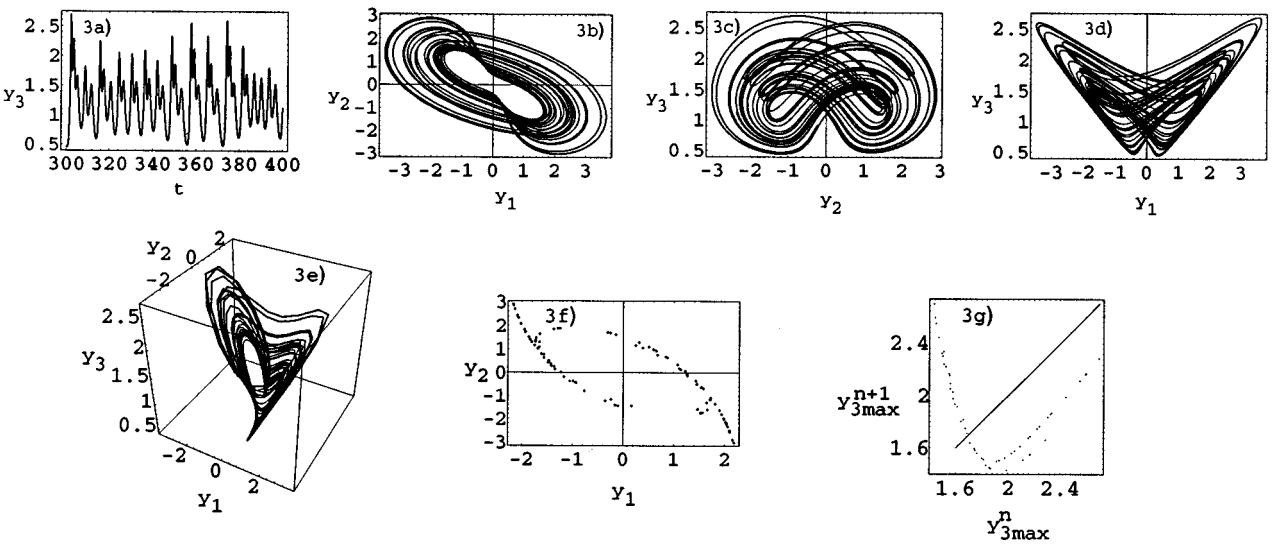

FIG. 3. The values of $\tilde{k}_1$, $\tilde{k}_2$, and $\tilde{k}_3$ are 1.35, 1, and 1/1.35, respectively. (a) y_3, exhibiting irregular motion, shown as a function of time after the trajectory is on the apparently chaotic attractor; (b) a projection of the attractor on the y_1-y_2 plane; (c) a projection of the attractor on the y_2-y_3 plane; (d) a projection of the attractor on the y_1-y_3 plane; (e) a three-dimensional plot of the attractor; (f) a Poincaré section of the attractor at $y_3=0$; (g) the return map of $y_{3\,\max}$ as well as a line segment of $y^{n+1}_{3\,\max}=y^{n}_{3\,\max}$.

$$\frac{d\tilde{y}_1(t)}{dt}=-\tilde{k}_1^2\,\exp[(\tilde{k}_1^2+\tilde{k}_2^2-\tilde{k}_3^2)t]\tilde{y}_2(t)\tilde{y}_3(t),$$

$$\frac{d\tilde{y}_2(t)}{dt}=\tilde{k}_2^2\,\exp[-(\tilde{k}_1^2+\tilde{k}_2^2+\tilde{k}_3^2)t]\tilde{y}_3(t)\tilde{y}_1(t), \qquad (4)$$

$$\frac{d\tilde{y}_3(t)}{dt}=-\tilde{k}_3^2\,\exp[(-\tilde{k}_1^2+\tilde{k}_2^2+\tilde{k}_3^2)t]\tilde{y}_1(t)\tilde{y}_2(t),$$

where $\tilde{y}_1(t)=y_1(t)\exp(\tilde{k}_1^2 t)$, $\tilde{y}_2(t)=y_2(t)\exp(-\tilde{k}_2^2 t)$, $\tilde{y}_3(t)=y_3(t)\exp(\tilde{k}_3^2 t)$.

We can assume without any significant loss of generality that

$$\tilde{k}_1^2>\tilde{k}_3^2. \qquad (5)$$

Then the only argument of the three exponentials that can change sign as the $\tilde{k}_i$'s are varied subject to the constraint, Eq. (5), is in the equation specifying $d\tilde{y}_3(t)/dt$. The argument equals zero when

$$\psi(\tilde{k}_1^2,\tilde{k}_2^2,\tilde{k}_3^2)=0, \qquad (6)$$

where $\psi(\tilde{k}_1^2,\tilde{k}_2^2,\tilde{k}_3^2)\equiv\tilde{k}_1^2-\tilde{k}_2^2-\tilde{k}_3^2$. Although $\tilde{k}_1^2$, $\tilde{k}_2^2$, and $\tilde{k}_3^2$ are three independent parameters, we can absorb one of them, say $\tilde{k}_2^2$, into a rescaling of the time, replacing $\tilde{k}_2^2 t$ by t (since $\tilde{k}_2^2$ has already been assumed to be greater than zero), if we simultaneously replace each of the $\tilde{k}_i^2$'s by their values in units of $\tilde{k}_2^2$. We thus do not lose any qualitative aspect of the solution by setting $\tilde{k}_2^2$ equal to 1 in Eqs. (4) or (2).

We shall now explore numerically the effect of crossing the boundary, $\psi(\tilde{k}_1^2,1,\tilde{k}_3^2)=0$, upon the character of the solution of Eqs. (2). We shall further limit the two-dimensional domain spanned by the two remaining parameters $\tilde{k}_1^2$ and $\tilde{k}_3^2$ by imposing the constraint $\tilde{k}_1^2=(\tilde{k}_3^2)^{-1}$. Equation (6) is then satisfied when $\tilde{k}_1^2$ equals 1.618 . . . , which is the golden section ratio Φ. Our numerical calculations, using MATHEMATICA, appear to demonstrate the presence of strange, chaotic attractors when $\psi(\tilde{k}_1^2,1,1/\tilde{k}_1^2)>0$. [The only attractors that we have observed when $\psi(\tilde{k}_1^2,\tilde{k}_2^2,\tilde{k}_3^2)<0$ have been simple limit cycles.]

Recalling that k_1, k_2, and k_3 in Eq. (1) represent the three sides of a triangle leads us to observe that the angle opposite the largest side, k_1, appears to be obtuse for the equations to produce a chaotic attractor. In order that the three wave numbers actually represent three sides of a triangle, we must further impose

$$\Phi^{1/2}<\tilde{k}_1<\Phi.$$

In Figs. 1(a)–1(e) we show properties of the attractor when $\tilde{k}_1=\Phi^{1/2}$. The trajectory of the attractor is a simple limit cycle that could be the edge of an orientable surface. The attractor is symmetric under the simultaneous replacement $y_1\to -y_1$, $y_2\to -y_2$, $y_3\to y_3$. As an example of the time evolution of a coordinate, we display $y_3(t)$ in Fig. 1(a), which is seen to execute simple periodic motion.

When we increase $\tilde{k}_1$ to the value 1.33, we observe in Figs. 2(a)–2(e) that the attractor is now a simple twisted closed loop that could define the edge of a Möbius strip, a nonorientable surface. Concomitant with this twist is the absence of the simple symmetry that we observed in our first case. In this case the y_3 coordinate exhibits the period-doubling characteristic of the route to chaos, which we appear to achieve, as depicted in Figs. 3(a)–3(g), when we further increase $\tilde{k}_1$ to the value 1.35.

In Fig. 3(a), the evolution of y_3 has become irregular. Figures 3(b)–3(e) exhibit the structure of the apparently chaotic attractor. In Fig. 3(f), a Poincaré section in the $y_3=0$ plane of the attractor depicted in Figs. 3(b)–3(e) is shown as an additional aid to visualizing the three-dimensional appearance of the attractor. Finally, in Fig. 3(g), we show a return map of $y_{3\max}$ as well as a line segment of $y^{n+1}_{3\max}=y^{n}_{3\max}$. [Each successive maximum $y^{n+1}_{3\max}$ of $y_3(t)$ is plotted as a

function of the previous maximum $y^n_{3\max}$.] If one were to imagine a continuous curve placed through this map, the magnitude of its slope over most of the domain would be greater than 1, as it also would be where the curve would intersect the line segment. As a result, there is no stable point. Indeed, there may be no multicycle stable points when this map is repeatedly iterated. These numerical results contain the standard indicators of the route to chaos, and so we believe that the cyclically symmetric equations, Eqs. (2) [or equivalently, Eqs. (1)] have chaotic attractors.

These equations merit further study. The connection between turbulence and vorticity dynamics has been much discussed. Here we have shown the characteristic unpredictability of turbulent dynamics, even at the level of the fundamental interaction of the incompressible Navier-Stokes equation: the triadic interaction of vorticity states, when the effects of the remaining states are modeled as a driver for the triad. The significance of the study lies in the rich intricacy of results produced by such a simple model. In particular, we have shown that the shape of the triangle of wave numbers of the three interacting helicity states affects the nature of the dynamics. When the angle opposite the largest side k_1 is obtuse, a chaotic attractor results; when acute, a simple limit cycle occurs. This boundary requires more precise delineation. Might there be some relevance here to the development of turbulence and the formation of coherent structures in fluids? One can increase gradually the number of modes whose detailed dynamics are retained. What effect does retaining additional modes have on the fluid's dynamics when a similar autonomous phenomenological driving term is maintained?

As a bonus, the cyclic symmetry of these equations suggests the potential for many applications. Other nonlinear cyclically symmetric sets of equations have been previously studied [8]. We have noted that, in addition to our equations being relevant to a Navier-Stokes fluid, they apply to the motion of a driven, dissipative rigid body. There have been and continue to be suggestions that equations leading to chaos may have the potential for explaining magnetic dynamos [9]. Exploring the possibility of constructing a (geo)magnetic dynamo based on the dynamics of our equations seems worthwhile.

I wish to thank my colleagues, Timothy T. Clark and Klaus Lackner, for constructive discussions; Rick Rauenzahn for a careful reading of this manuscript; and my son, Ari, for the proof that the complex roots of Eq. (3) have a positive real part. This work was supported by the U.S. Department of Energy.

[1] A. J. Chorin, *Vorticity and Turbulence* (Springer-Verlag, New York, 1994).

[2] S. Chandrasekhar and P. C. Kendall, Astrophys. J. **126**, 457 (1957).

[3] Different phasing assumptions also can lead to chaos, but with a far less symmetric set of equations and concomitant fewer potential applications. For example, see J.-M. Wersinger, J. M. Finn, and E. Ott, Phys. Rev. Lett. **44**, 453 (1980).

[4] R. H. Kraichnan, J. Fluid Mech. **59**, 745 (1973).

[5] F. Waleffe, Phys. Fluids A **4**, 350 (1992).

[6] C. M. Bender and S. A. Orszag, *Advanced Mathematical Methods for Scientists and Engineers* (McGraw-Hill, New York, 1978), pp. 202–204.

[7] J. V. Uspensky, *Theory of Equations* (McGraw-Hill, New York, 1948), pp. 84–86.

[8] R. M. May and W. J. Leonard, SIAM J. Appl. Math. **29**, 243 (1975); F. H. Busse and K. E. Heikes, Science **208**, 173 (1980).

[9] K. A. Robbins, Proc. Cambridge Philos. Soc. **82**, 309 (1977); S. Childress and A. D. Gilbert, *Stretch, Twist, and Fold: The Fast Dynamo* (Springer, Berlin, 1995).